The Thermochemical Properties of Ammonium Exchanged Erionite

T. J. WEEKS, JR., C. L. ANGELL AND A. P. BOLTON

*Molecular Sieve Department and Central Scientific Laboratory,
Union Carbide Corporation, Tarrytown Technical Center,
Tarrytown, New York 10591*

The thermochemical properties of ammonium exchanged erionite are examined by thermal analyses, infrared spectroscopy, and high temperature X-ray diffractometry.

INTRODUCTION

The thermochemical properties of ammonium exchanged type Y zeolite have been extensively investigated (*1–3*) because of its efficacy in catalysis. Erionite and type T zeolite have recently attracted interest as shape selective catalysts (*4,4*a, *5*). However, data on the ammonium exchanged forms of these two zeolites are fragmentary. This is a study of the changes which occur upon thermal treatment of ammonium exchanged erionite as determined by thermal analyses, infrared spectroscopy and X-ray diffractometry.

EXPERIMENTAL SECTION

Materials

The starting material was a mineral erionite from the western United States which had been repeatedly exchanged with NH_4Cl at reflux temperature. The zeolite had the following composition:

	Wt%		Molar ratio
Al_2O_3	17.2	SiO_2/Al_2O_3	7.06
SiO_2	71.5	K_2O/Al_2O_3	0.22
K_2O	3.7	$(NH_4)_2O/Al_2O_3$	0.79
$(NH_4)_2O$	6.5		
Na_2O	0.1		
$MgO + FeO$	0.9		

Procedure

Thermal analyses. DTA data were obtained on a Stone Tracor Model 202 differential thermal analyzer with a dynamic gas flow sample holder. When dry air was used as a purge gas the following instrument conditions applied: heating rate = 10°C/min, flow rate = 23.6 ml/min; gain = 800 μV; sample wt = 150 mg; reference = 250 mg Al_2O_3; differential thermocouple = Platinel II. With a dry helium purge the same conditions were maintained except the gain was changed to 500 μV for increased sensitivity. In this equipment the purge gas passes directly through the sample and reference cells. It is our experience with ammonium exchanged zeolites that if the purge gas passes only over the sample holder, as with many instruments, a thermogram can result which may be misleading.

A DuPont Model 950 thermogravimetric analyzer was used under the following conditions: dry air purge = 37.6 ml/min; heating rate = 10°C/min; sample wt = 25.59 mg.

Infrared analyses. Spectra were recorded on self-supporting wafers in a cell similar to that previously described (*6*). Samples were heated in flowing dry air at 100°C increments, following evacuation at

room temperature. All spectra were recorded at room temperature on one thermally cycled sample. The hydroxyl stretching region was scanned with a Perkin-Elmer Model 112 single beam spectrophotometer on a 5 mg wafer. The mid-frequency and framework regions were run with a Perkin-Elmer Model 225 double beam spectrophotometer on 7 mg and 5 mg pellets, respectively.

X-Ray diffraction. A Materials Research Corporation high temperature diffractometer employing Cu $K\alpha$ radiation was used. Scan rate over a 2θ range of 4 to 44° was 1°/min. The sample was deposited as an aqueous slurry on the platinum sample stage and vacuum dried. An internal standard was not employed. Temperature control was achieved with the heated sample stage and auxiliary side heaters. A dry helium purge was used. In several instances air purged samples were taken from the TGA apparatus, hydrated, and scanned on a Norelco diffractometer with a graphite monochromator.

The following 12 indices were used to calculate cell constant data (7). The 2θ values at room temperature are: h,k,l (2θ); 1,1,0 (13.38); 2,0,0 (15.45); 2,0,1 (16.52); 1,2,0 (20.50); 1,2,1 (21.32); 3,0,0 (23.30); 1,2,2 (23.70); 1,0,4 (24.90); 2,2,0 (26.95); 4,0,0 (31.20); 4,0,1 (31.75); 4,0,2 (33.40). The computer program used in calculating cell constants from the 2θ data is essentially an extrapolation procedure based on Cohen's least squares method; the precision was estimated at ±0.04 Å. At higher temperatures (700°C) only six of the above peaks are intense enough for analysis, hence the uncertainty is greater (±0.1 Å). The cell indices and 2θ values used at 700°C are 1,1,0 (13.60); 2,0,0 (15.72);
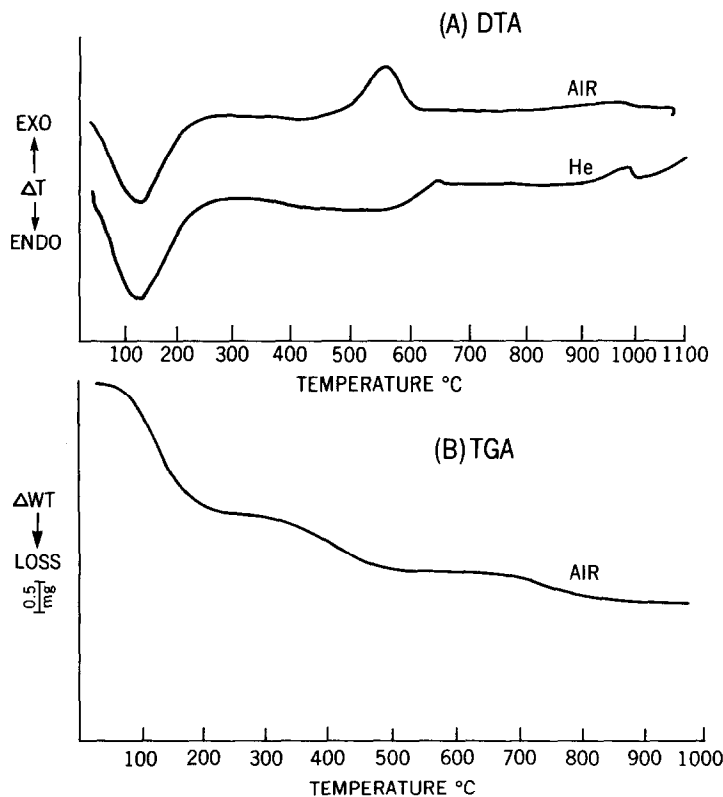

FIG. 1. Thermograms of ammonium exchanged erionite.

1,2,0 (20.90); 1,2,1 (21.70); 1,0,4 (24.72); 2,2,0 (27.45).

RESULTS AND DISCUSSION

The structures of erionite and type T have been characterized (8,9). The framework is essentially composed of cancrinite cages connected through double six rings forming a column. The columns are connected, in the erionite structure, to form supercages with elliptical pore openings 3.6 × 5.2 Å. Although the stacking in type T differs slightly, the effective pore size is the same as in erionite. The differences in catalytic activity and structural stability of erionite and type T have been discussed previously (4). It is likely that the properties presented here for ammonium exchanged erionite also generally apply to ammonium exchanged T.

Thermal analysis. Data are presented in Fig. 1. The DTA in air shows a sharp endotherm at 135°C due to desorption of water and a sharp exotherm at 550°C due to ammonia oxidation. There may be a shallow endotherm at 425°C which would indicate that some ammonia is desorbed prior to oxidation. Although it is not apparent from Fig. 1, a slight dehydroxylation endotherm was noted at 750°C when instrument sensitivity was increased fivefold. An exotherm can be seen at 950°C which was shown to be due to crystal collapse by X-ray diffraction analysis. When the heating rate was increased to 20°C/min, the exotherm at 550°C became a doublet with a shoulder at 460°C and a peak at 575°C.

With a helium purge water desorbed at 125°C, and ammonia desorbed between 400 and 550°C as indicated by the endotherms in Fig. 1. The small exotherm at 625°C was observed on repeated analyses, even after purging for 24 hr at room temperature with helium. Thus it is unlikely that this exotherm is an artifact. It may be due to proton rearrangement in the zeolite (2). It should be pointed out that a slight

perturbation in the thermogram near 400°C is due to a phase change in the nickel sample holder. This phase change occurs at 353°C in an isothermal system.

The TGA in air shows three distinct steps corresponding to loss of water (RT → 250°C), deammoniation (300 → 550°C), and dehydroxylation (650 → 850°C). Loss of ammonia was 4.66 wt% (cf. 4.25 wt% by chemical analysis) and the weight loss due to dehydroxylation was 2.12 wt% (cf. 2.25 wt% by chemical analysis). Although these results would indicate that some water loss occurs during deammoniation, the experimental
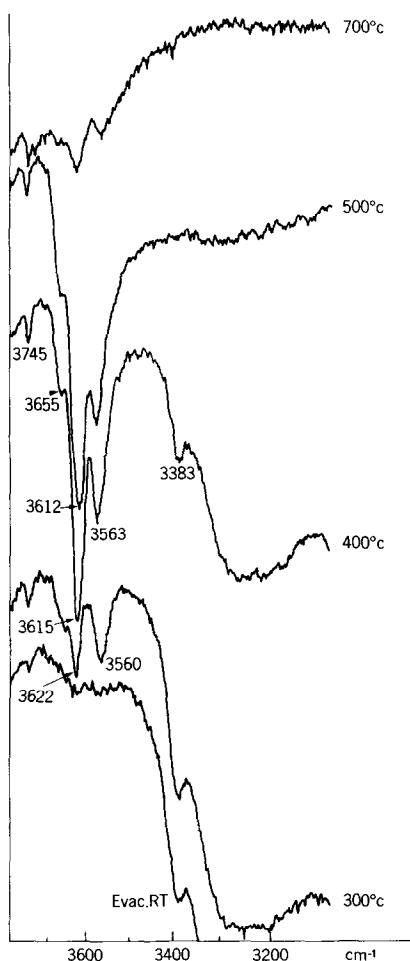

FIG. 2. Infrared spectra of hydroxyl stretching region for ammonium exchanged erionite as function of temperature.

error of ± 0.2 wt% in the $(NH_4)_2O$ analysis makes this a tenuous conclusion.

Infrared spectra. One publication has discussed the infrared spectrum of the hydroxyl stretching region of ammonium exchanged erionite and the interaction of these hydroxyls with organic compounds (*10*). In the present study it was found that zeolitic water can be removed by evacuation at room temperature (Fig. 2) and this allows the 3745 cm^{-1} band, due to amorphous material, to become evident. At 300°C bands at 3622, 3560 cm^{-1} and a shoulder at 3655 cm^{-1} become visible. Upon increasing the temperature, these bands shift to 3615 and 3563 cm^{-1}, respectively, as previously reported (*10*). Hydroxyl concentration is at a maximum between 500 and 600°C but is still evident

at 700°C. The infrared region from 1900 to 1000 cm^{-1}, shown in Fig. 3, also confirms that water (1635 cm^{-1}) is lost upon room temperature evacuation and that the ammonium cation (1420 cm^{-1}) is removed by 500°C. Frequency variations in several framework overtone vibrations can also be seen. Changes in the infrared framework region as a function of temperature are shown in Fig. 4. A room temperature spectrum of the framework region has been published previously (*11*). An increase in temperature from ambient to 500°C results in the following bands shifting in frequency to the positions indicated: $780 \rightarrow 795$ cm^1, $630 \rightarrow 640$ cm^{-1}, $570 \rightarrow 580$ cm^{-1}, 1100 cm^{-1} $\rightarrow$ higher. In addition the 550 cm^{-1} band disappears and the band at 720 cm^{-1} decreases in inten-
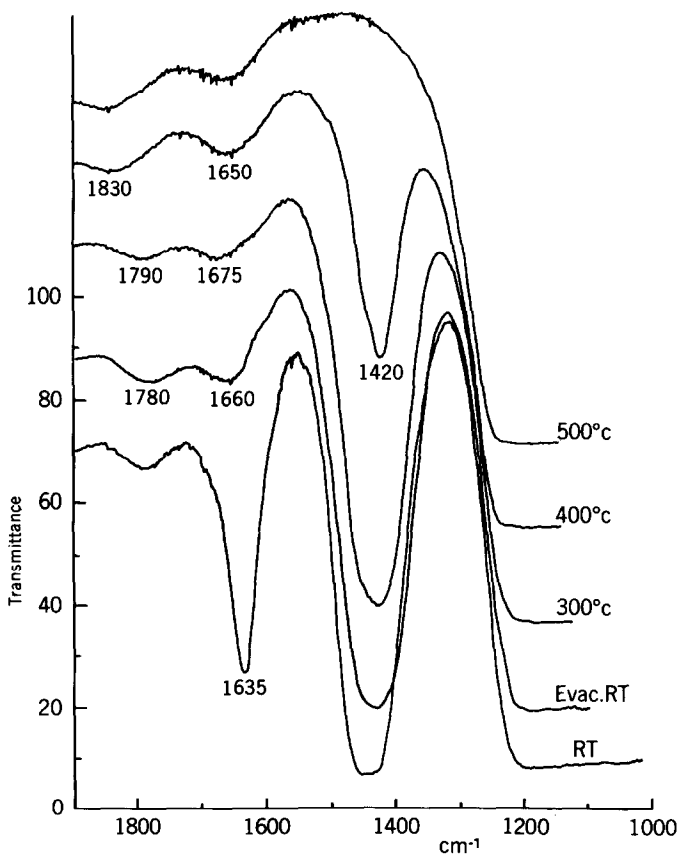

FIG. 3. Effect of temperature on the infrared region between 1800 and 1000 cm^{-1} of ammonium exchanged erionite.
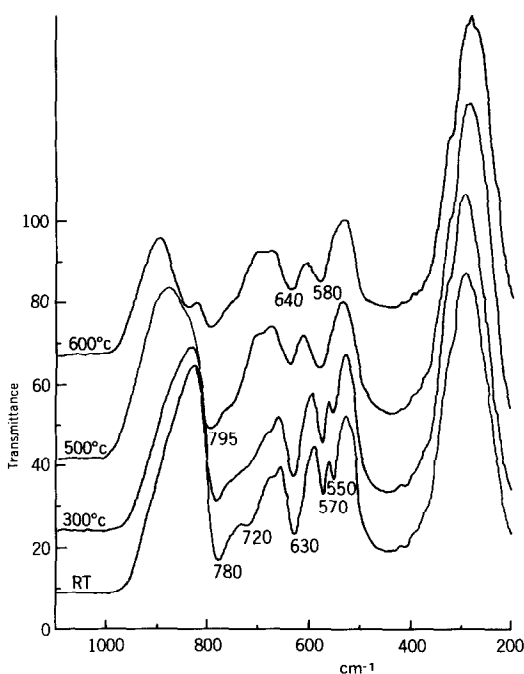
FIG. 4. Effect of temperature on the infrared spectra of the framework region of ammonium exhanged erionite.

sity. These changes appear to be associated with the loss of ammonium cation. At 600°C, which is the onset of dehydroxylation a new band at 840 cm^{-1} appears. The same changes were evident with helium activated samples. The increase in frequency of certain vibrations may indicate that the zeolite framework is becoming more siliceous during calcination by the elimination of alumina. This is suggested by a study in which the silica to alumina ratios of various zeolites are plotted versus particular framework vibrations (12). It should be emphasized that when conducting calcination experiments in an infrared cell, self-supporting wafers rather than KBr pellets must be used; otherwise salt loading will occur (1) and thus prevent observation of some of the above changes.

X-Ray diffraction data. An internal standard was not employed in the MRC diffractometer due to the possibility of high temperature substitution reactions. Also,

dilution would tend to diminish the intensity of the signal. The same specimen was used and thermally cycled to prevent errors due to a changing sample geometry. Table 1 presents the changes in cell constants as a function of temperature in the MRC instrument. In one case a sample was heated directly to 600°C and its pattern was similar to that of the cycled zeolite. The cell constants for the starting ammonium exchanged erionite were determined on a standardized Norelco instrument and were $a_0 = 13.25$ Å, $c_0 = 15.07$ Å. Cell constants for an erionite ore from the western United States are $a_0 = 13.26$ Å, $c_0 = 15.12$ Å (7). The difference between the values found at room temperature in helium or vacuum in Table 1 and those for the Norelco instrument indicate the absolute error between the two diffractometers caused by sample geometry. The relative error between readings on the MRC camera is estimated to be less than 0.04 Å. It can be seen that the cell constants remain unchanged from room temperature through 500°C. This is in marked contrast to the framework infrared spectra which show dramatic changes accompanying loss of ammonia. At 600°C there is a slight decrease in a_0, both at tem-

TABLE 1

CELL CONSTANTS OF NH_4^+ ERIONITE AT VARIOUS TEMPERATURES IN HELIUM

Temp (°C)	Time (hr)	a_0 (Å)	c_0 (Å)
R T	64 Vac.	13.16	15.01
R T	2 He	13.21	15.07
200	2 He	13.19	15.00
300	2 He	13.19	15.06
R T	16 He	13.16	15.03
400	2 He	13.15	15.09
500	2 He	13.14	15.11
R T	3 He	13.14	15.03
600	2 He	13.05	15.13
R T	16 He	13.08	15.03
700	2 He	13.0	15.2
800	2 He	13.0	15.3

perature and upon cooling. The small in-
crease in c_0 at temperature appears revers-
ible upon cooling. As the crystal degrades
at 800°C there is a further decrease in a_0
and increase in c_0. These values have a
greater uncertainty due to the fewer
number of peaks in the diffraction pattern.
Overall it can be seen that cell constant
changes accompanying crystal collapse are
not dramatic.

Figures 5A and 5B present the diffrac-
tion patterns at several points in the cycle

shown in Table 1. It should be pointed out
that for the cell constant calculations the
sensitivity was fourfold that shown in the
figures. There were slight differences in
patterns between a hydrated sample run on
the Norelco instrument and the evacuated
and helium purged sample run on the
MRC instrument which is shown in Fig.
5A. In the former a triplet instead of the
doublet at 31.5° was visible. This is pos-
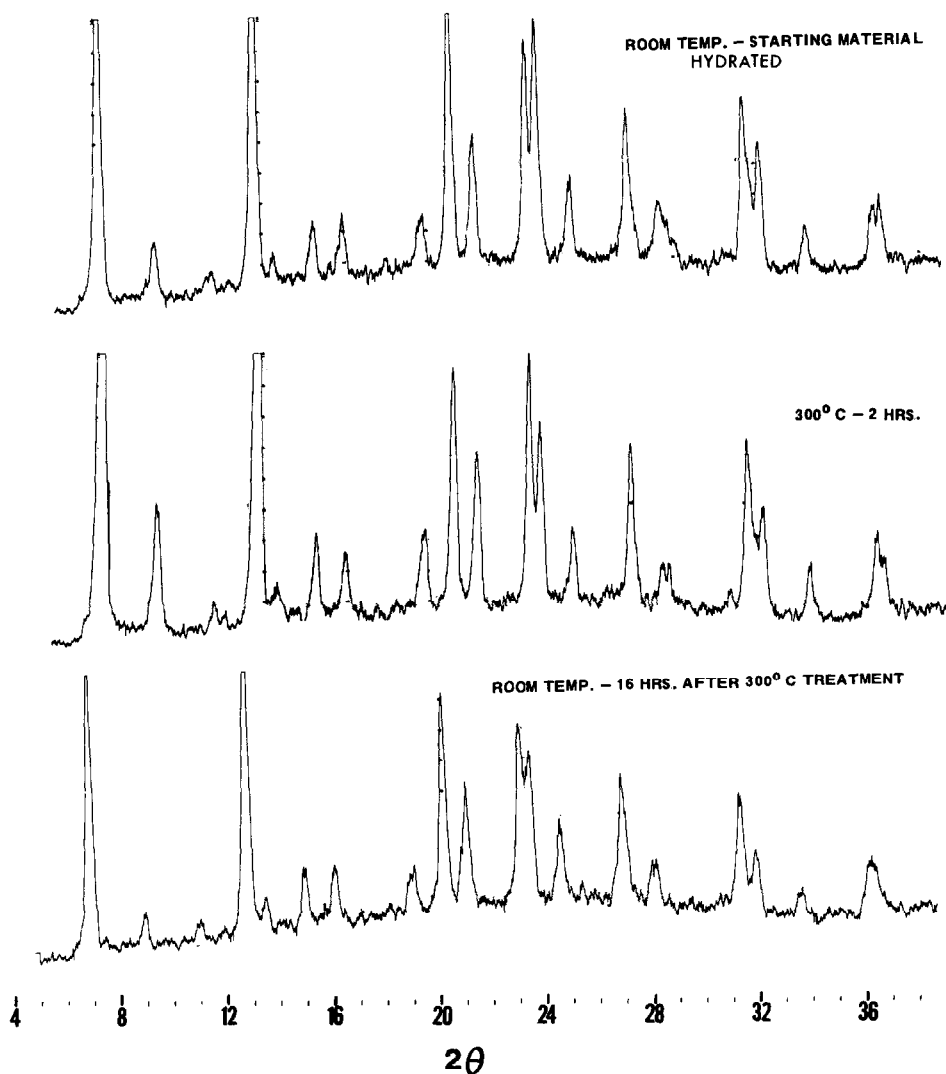sibly due to difference in sample hydration
levels since zeolite removed from the

FIG. 5A. X-Ray diffraction patterns of ammonium exchanged erionite at various temperatures with a helium purge.

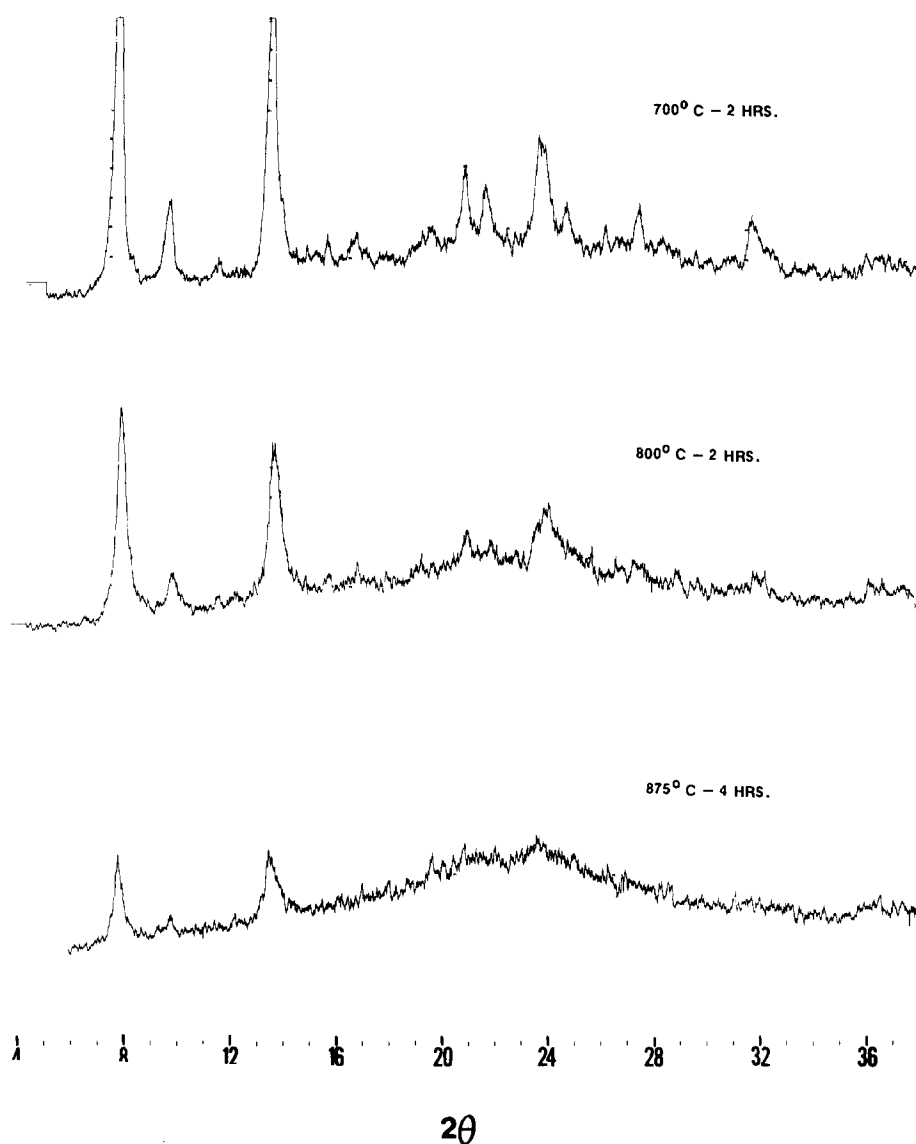700° C — 2 HRS.

800° C — 2 HRS.

875° C — 4 HRS.

2θ

Fig. 5B. X-Ray diffraction patterns of ammonium exchanged erionite at various temperatures with a helium purge.

TGA with an air purge and hydrated also showed the triplet at 31.5° present until 400°C. The diffraction pattern of the sample in the high temperature camera showed changes at 300°C which were the inversion of a doublet at 23.5° and in increase in intensity of the 9.6° peak. The intensity of the 9.6° (1,0,1) peak decreased upon cooling to room temperature. By 700°C major changes in the X-ray diffrac-tion pattern have occurred as evidenced by the decrease in intensity of most peaks shown in Fig. 5B. The sample was almost amorphous by 875°C. Specimens taken from the TGA and subsequently hydrated had patterns similar to those obtained with the high temperature camera. However, there was about a 100°C temperature lag between these two methods. That is, a sample taken from the TGA at 800°C had

a pattern similar to that of the static system at 700°C.

CONCLUSIONS

The effect of temperature on ammonium exchanged erionite as determined by thermal analyses, infrared spectroscopy and high temperature X-ray diffractometry has been presented. Thermal analyses show that water loss, deammoniation, and dehydroxylation occur in discrete steps with an ammonia oxidation exotherm occurring at 550°C. Isothermal infrared analyses show that water can be removed by evacuation at room temperature. Hydroxyl stretching bands occur at 3612 and 3563 cm^{-1}; maximum hydroxyl concentration is achieved between 500 and 600°C. Some hydroxyl bands are still evident at 700°C. Ammonia removal is accompanied by dramatic changes in the framework region of the infrared spectrum. Isothermal X-ray diffraction data show that the cell constants are remarkably stable and that extensive crystal degradation occurs by 800°C.

REFERENCES

1. Breck, D. W., "Zeolite Molecular Sieves." Wiley, New York, 1974.
2. Bolton, A. P., and Lanewala, M. A., *J. Catal.* **18**, 154 (1970).
3. Kerr, G. T., *Advan. Chem. Ser.* **121**, 219 (1973).
4. Chen, N. Y., *in* "Catalysis" (J. W. Hightower, Ed.), Vol. 2. Amer. Elsevier, New York, 1973.
4a. Chen, N. Y., and Garwood, W. E., *Advan. Chem. Ser.* **121**, 575 (1973).
5. Chen, N. Y., Maziuk, J., Schwartz, A. B., and Weisz, P. S., *Oil Gas J.* **66**, 154 (1968).
6. Angell, C. L., and Shaffer, P. C., *J. Phys. Chem.* **69**, 3463 (1965).
7. ASTM File card 12-275.
8. Bennett, J. M., and Gard, J. A., *Nature (London)* **214**, 1005 (1967).
9. Kawahara, A., and Curien, H., *Bull. Soc. Fr. Mineral. Cristallogr.* **92**, 250 (1969).
10. Best, D. F. and Larson, R. W., and Angell, C. L., *J. Phys. Chem.* **77**, 2183 (1973).
11. Eberly, P. E., Jr., Laurent, S. M., Robson, H. E., *U.S. Pat.* 3,591,488 (1971).
12. Flanigen, E. M., Khatami, H., Szymanski, H. A., *Advan. Chem. Ser.* **101**, 201 (1971).